

Supporting Information for

Elucidating a dissolution-deposition reaction mechanism

by multimodal synchrotron X-ray characterization in aqueous Zn/MnO₂ batteries

Varun R Kankanallu ^a, Xiaoyin Zheng ^a, Denis Leschev ^b, Nicole Zmich ^a, Charles Clark ^a,
Cheng-Hung Lin ^{a,b}, Hui Zhong ^d, Sanjit Ghose ^b, Andrew Kiss ^b, Dmytro Nykypanchuk ^c, Eli Stavitski ^b,
Kenneth J. Takeuchi ^{a,e,f,g}, Amy C. Marschilok ^{a,e,f,g}, Esther S. Takeuchi ^{a,e,f,g},
Jianming Bai ^b, Mingyuan Ge ^{b,*}, Yu-chen Karen Chen-Wiegart ^{a,b,*}

^a Department of Materials Science and Chemical Engineering, Stony Brook University, Stony Brook, NY, 11794, USA

^b National Synchrotron Light Source II, Brookhaven National Laboratory, Upton, NY, 11973, USA

^c Center for Functional Nanomaterials, Brookhaven National Laboratory, Upton, NY, 11973, USA

^d Department of Joint Photon Sciences Institute, Stony Brook University, NY, 11790, USA

^e Energy and Photon Sciences Directorate, Brookhaven National Laboratory, Upton, NY 11973

^f Department of Chemistry, Stony Brook University, Stony Brook, NY, 11794

^g Institute of Energy Sustainability and Equity, Stony Brook University, Stony Brook, NY, 11794

Corresponding Author: Karen.Chen-Wiegart@stonybrook.edu; mingyuan@bnl.gov

Supplementary Figures

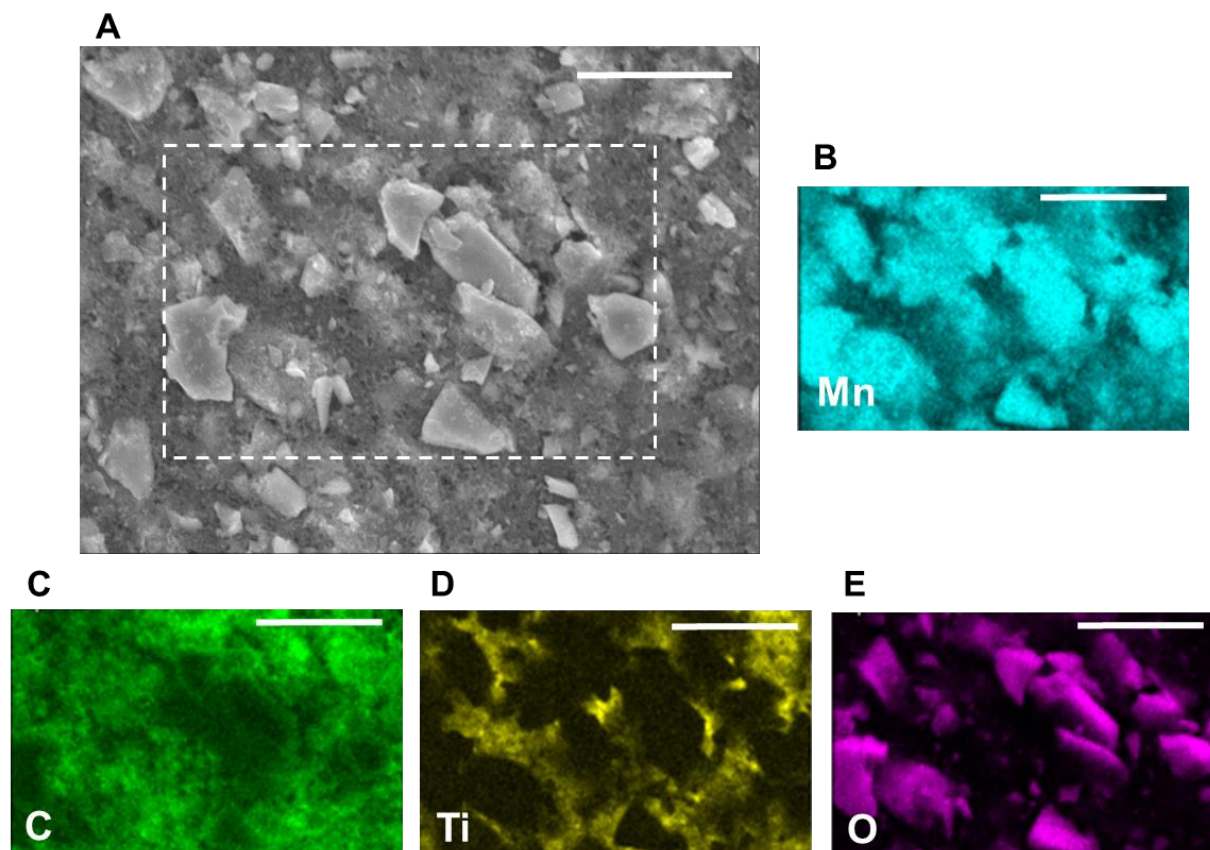


Fig. S 1 A SEM image and elemental mapping from the energy dispersive X-ray spectroscopy (EDX) analysis of **B** Mn, **C** carbon, **D** Ti, and **E** oxygen elements of pristine β - MnO_2 electrode. The particle size of the particles varies between 1-10 μm . The scale bar represents 10 μm .

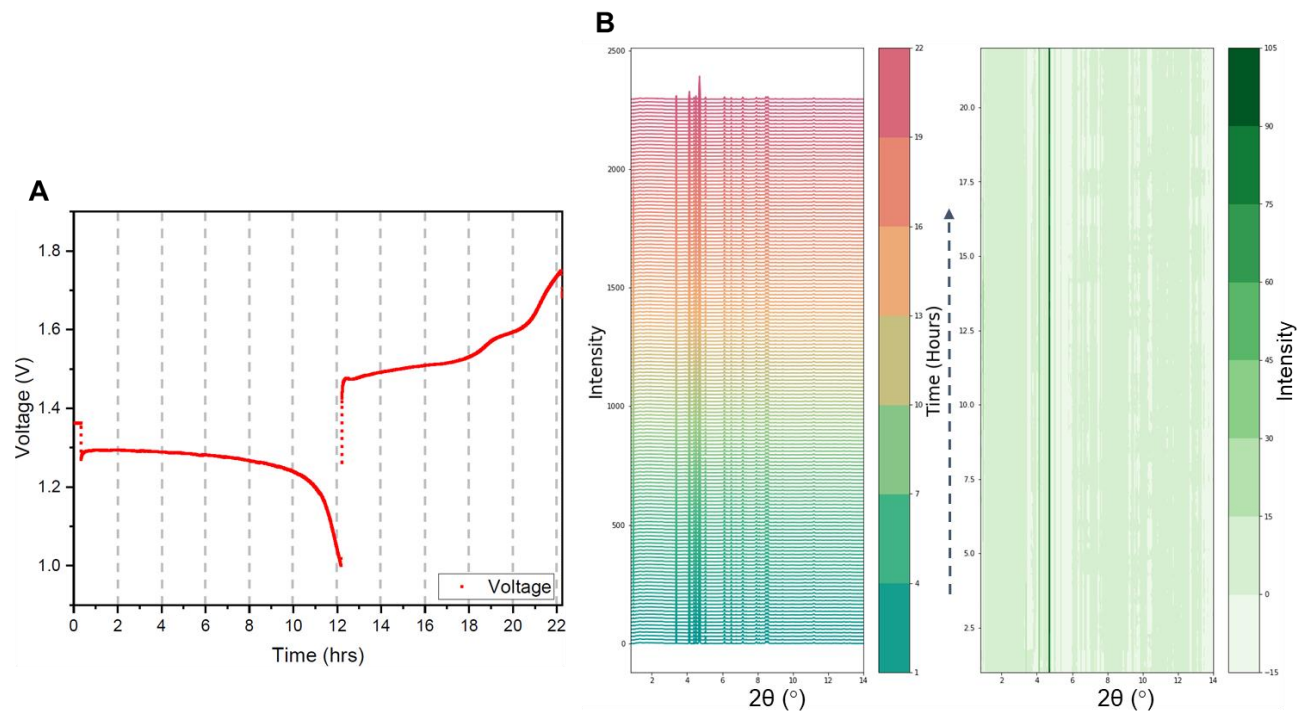


Fig. S 2 A *Operando* X-ray diffraction studies on β - MnO_2 electrode cycled between 1.0-1.75 V. **A** represents the electrochemical potential as a function of time and **B** is the corresponding waterfall plots of the *operando* scans

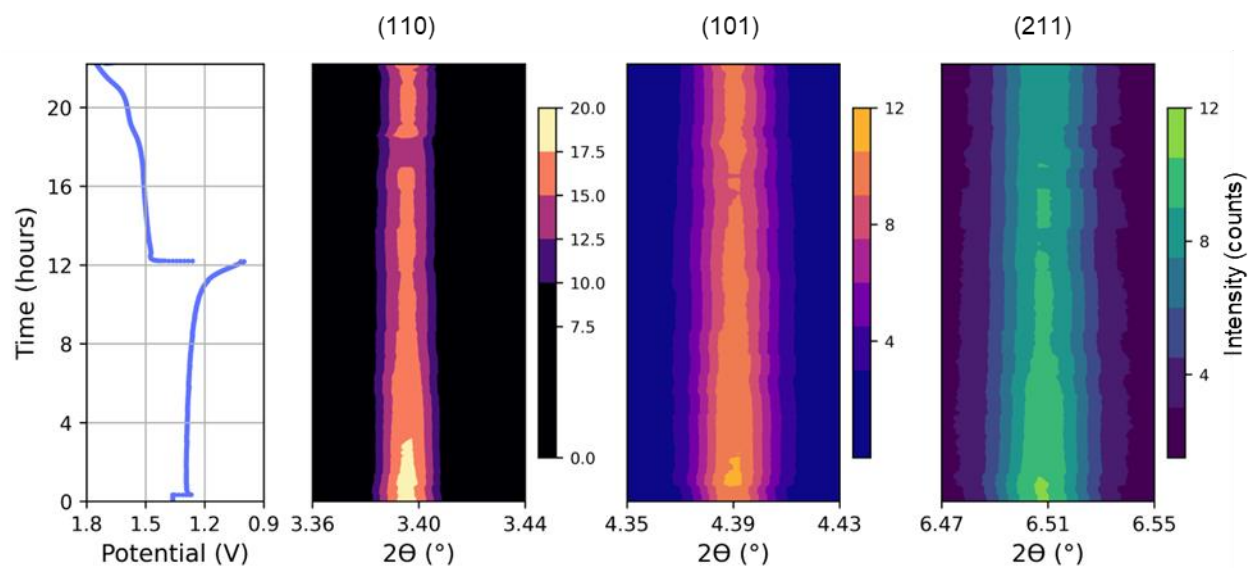


Fig. S 3 The galvanostatic discharge -charge profile for the first cycle and the corresponding waterfall plot of the three prominent crystal planes (110), (101) and (211) of β -MnO₂. Gradual decrease in the peak intensity during discharge is visible.

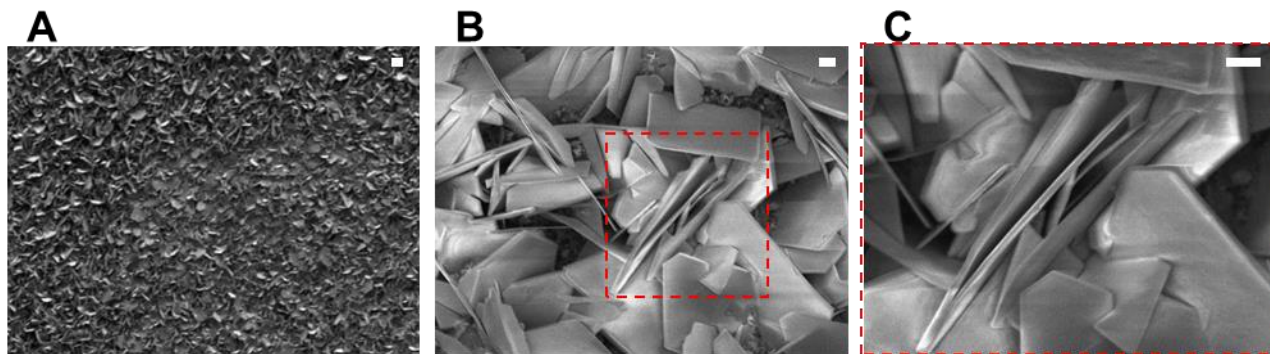


Fig. S 4 SEM images of ZHS precipitates growing over the β - MnO_2 electrode during the discharge half cycle. Scale bar in **A** is 10 μm , and in **B**, **C** is 1 μm .

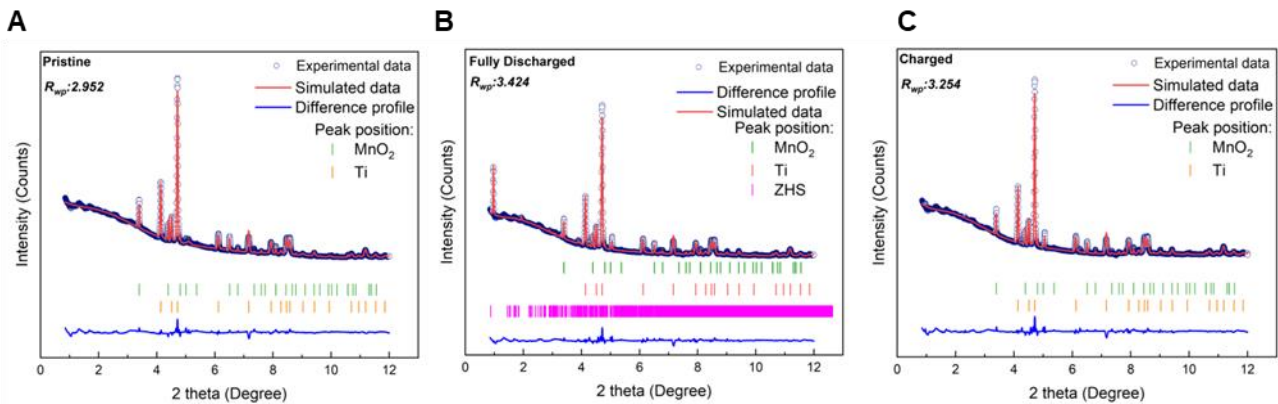


Fig. S 5 Rietveld refinement results of *operando* X-ray diffraction samples at different states: **A** pristine, **B** fully discharged, and **C** charged.

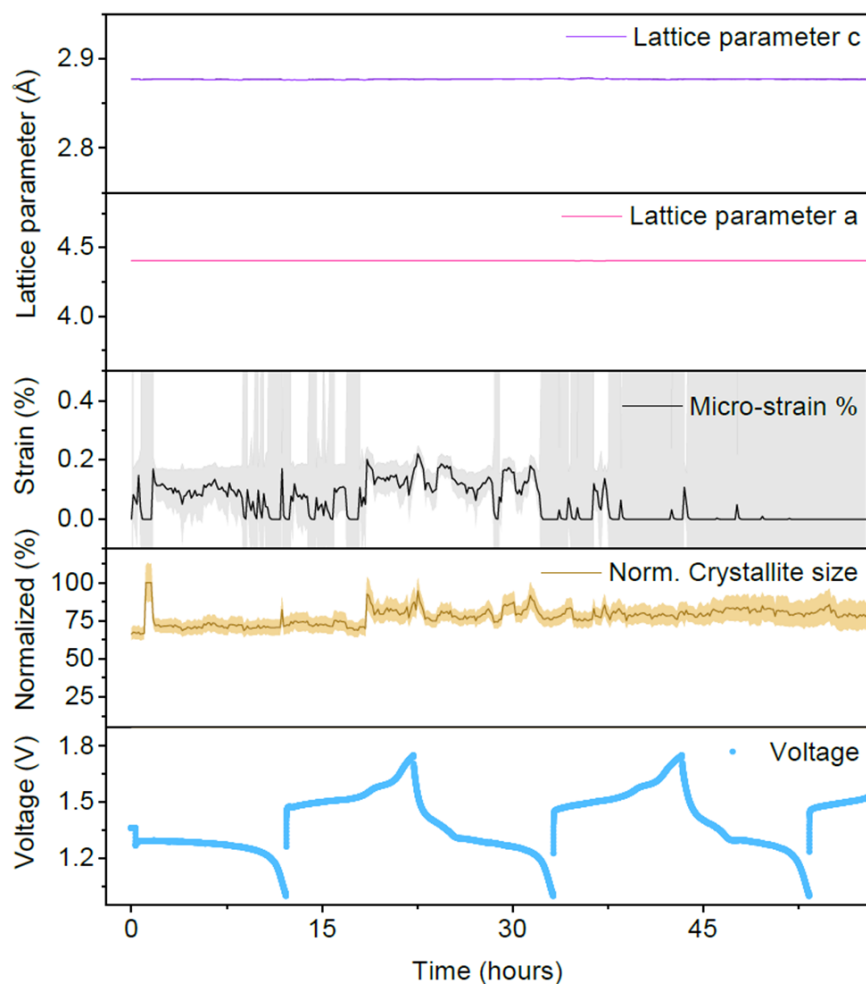


Fig. S 6 The normalized crystallite size, μ -strain percentage, lattice parameter *a* and *c*. The lighter shade in crystallite size and micro-strain indicates the error bars from the fitting. The error bars for the lattice parameter fitting are too small to be displayed here, $\sim 10^{-4}$ Å.

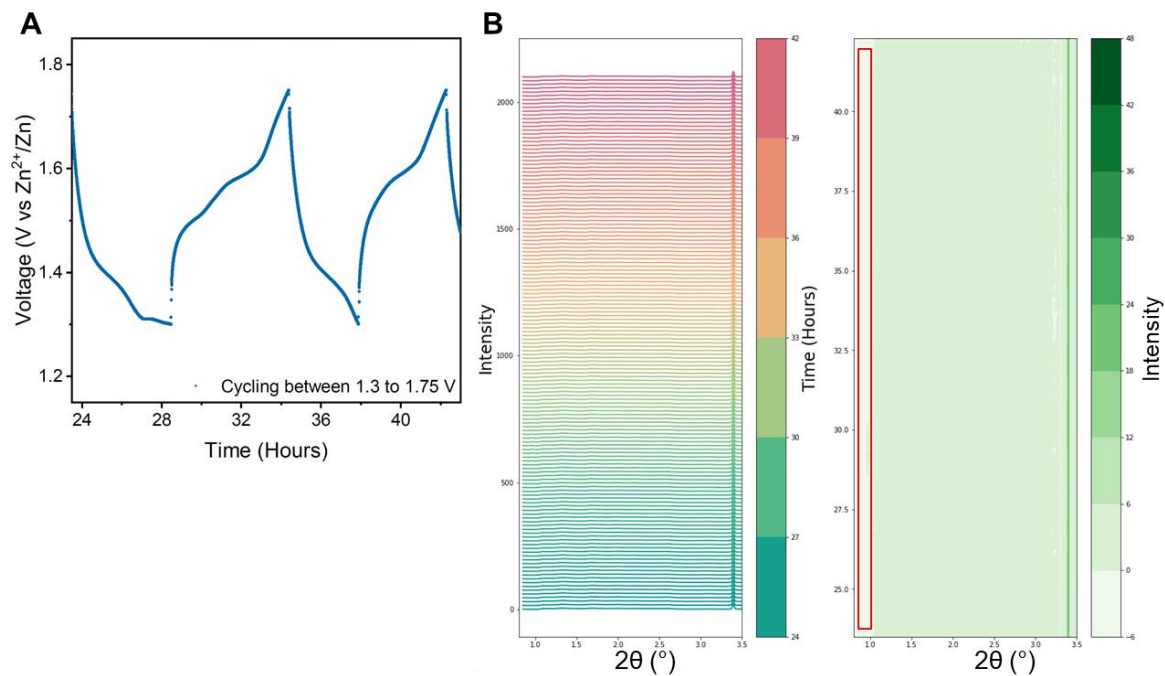


Fig. S 7 Operando X-ray diffraction studies on β -MnO₂ electrode cycled between 1.3-1.75 V after an initial activation cycling between 1-1.75 V. **A** represents the electrochemical potential as a function of time and **B** is the corresponding waterfall plots of the *operando* scans. The red rectangle indicates the position corresponding to the ZHS phase, which is absent in this cycling voltage range.

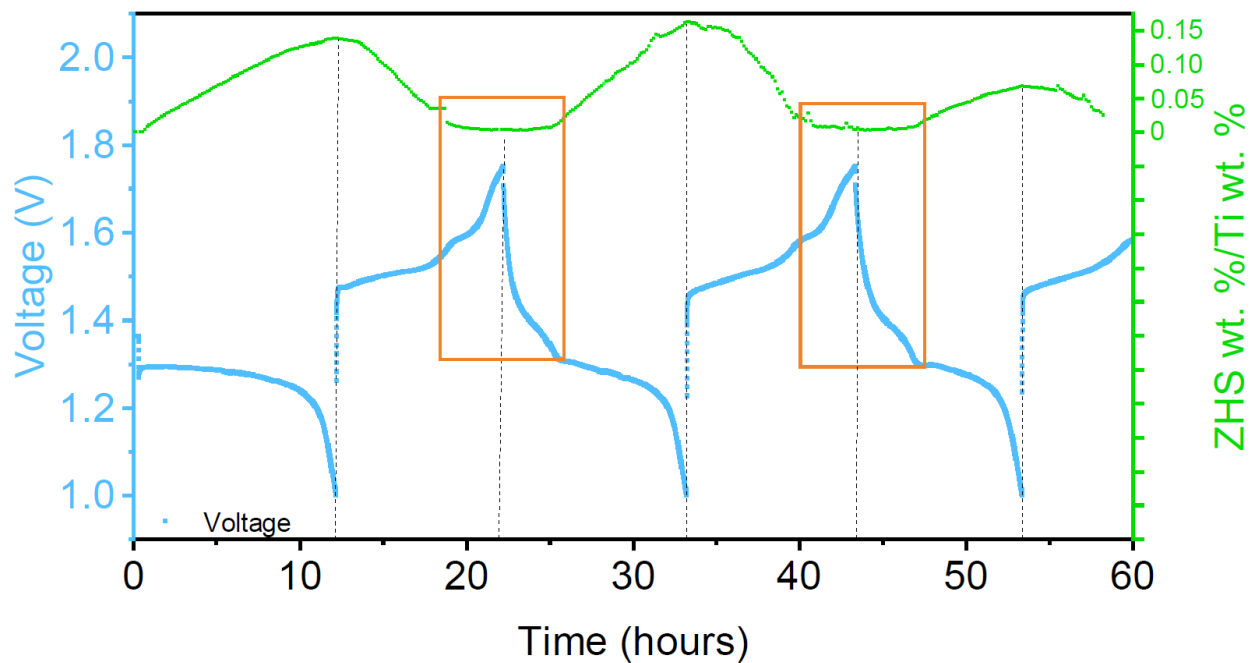


Fig. S 8 Relative ZHS weight plotted with respect to the electrochemical potential for the first 60 hours (~ 3 cycles), corresponding to the operando diffraction results as shown in **Fig. 2C**. The orange boxes indicate the electrochemical potential range ~ 1.3-1.75 V, in which there is a negligible change in the ZHS weight fraction.

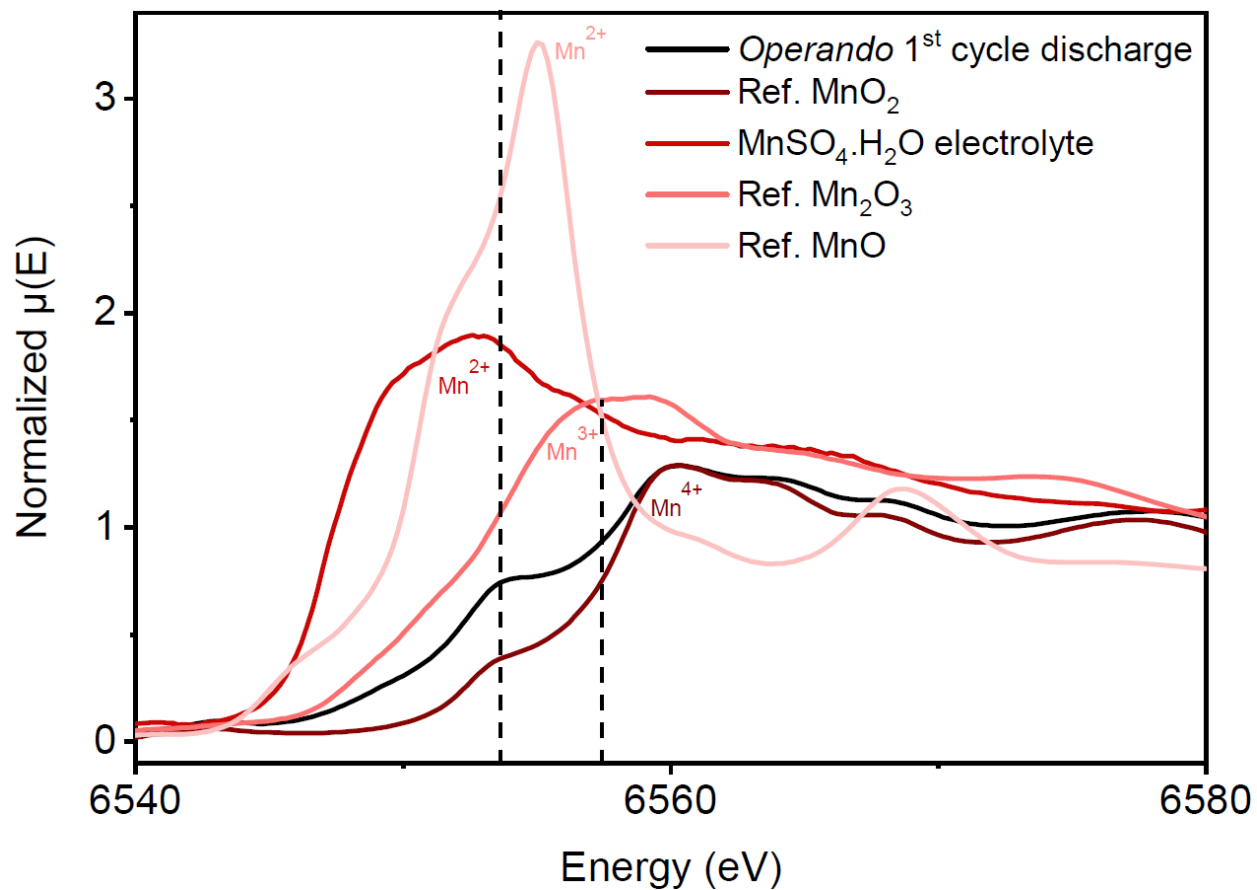


Fig. S 9 XANES spectra of *operando* 1st cycle discharge state, MnO₂, MnSO₄.H₂O, MnO, and Mn₂O₃ across the Mn-K edge. The dotted lines indicate the contribution of the Mn²⁺ ions towards the pre-edge feature in the *operando* 1st cycle discharge XANES spectra.

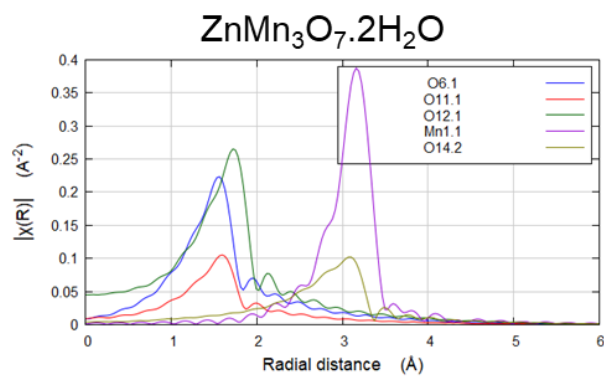
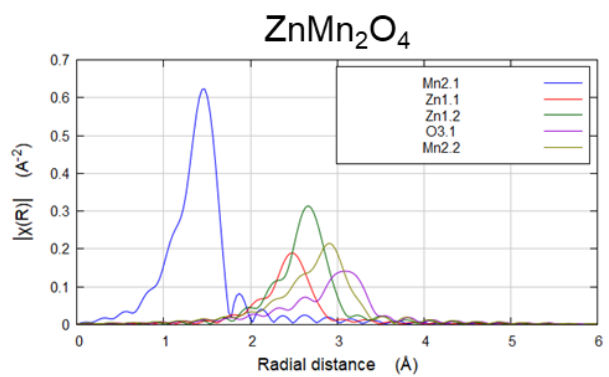
A**B**

Fig. S 10 FEFF calculated single-scattering paths for ZnMn₃O₇·2H₂O and ZnMn₂O₄.

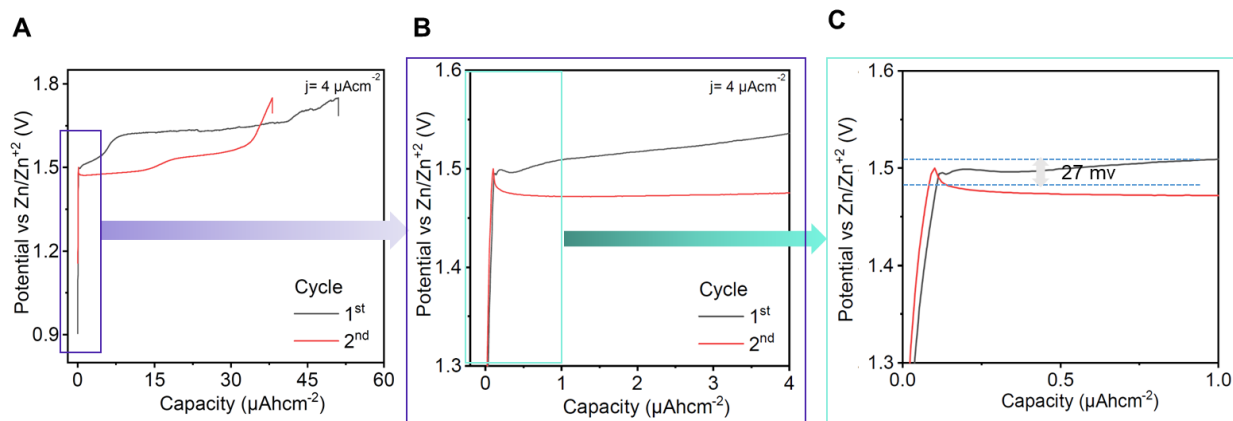


Fig. S 11 Nucleation overpotential of the Zn-Mn complex over the carbon black electrode. **A** The first two charge profiles of the cell indicate that the second charge scan has a lower overpotential in comparison with the first. **B** and **C** represent the zoom-in view on the x-axis of **A**, to indicate the overpotential.¹

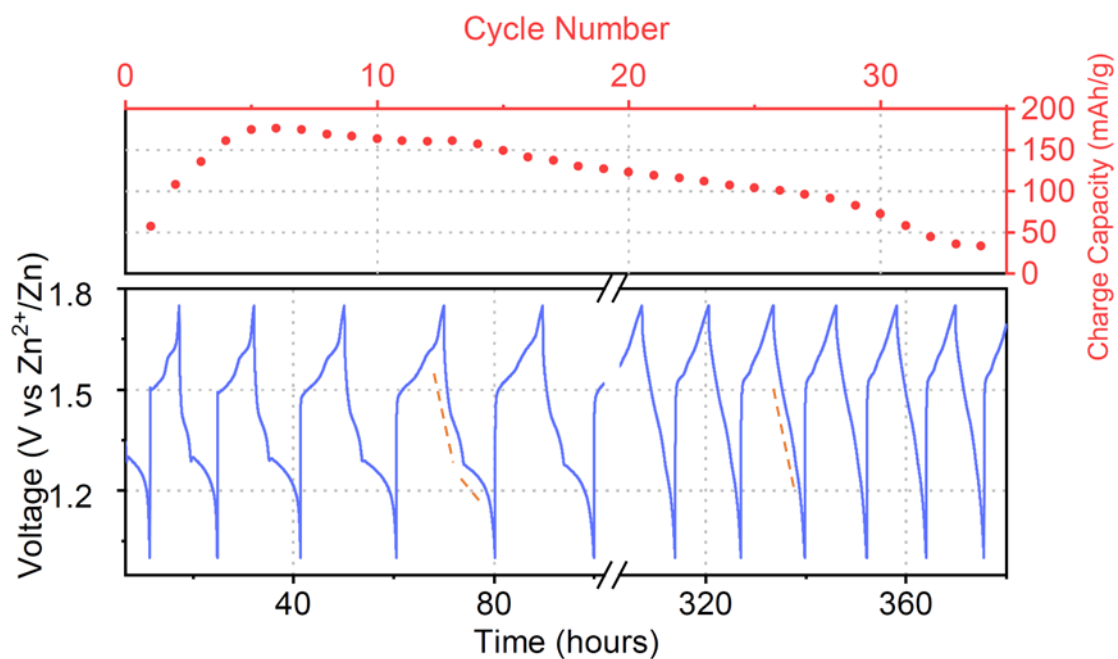


Fig. S 12 Extended cycling study of aqueous Zn/ β -MnO₂ battery at 0.1 C indicating the transition from a crystalline to amorphous phase.

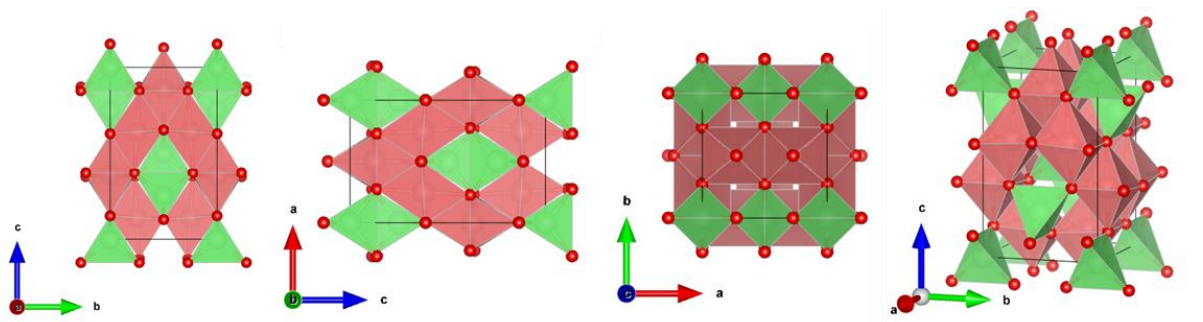


Fig. S 13 Crystallographic representation of the ZnMn₂O₄ crystal with views in three different orientations, along a, b, c axes respectively, and a 3D view. ²

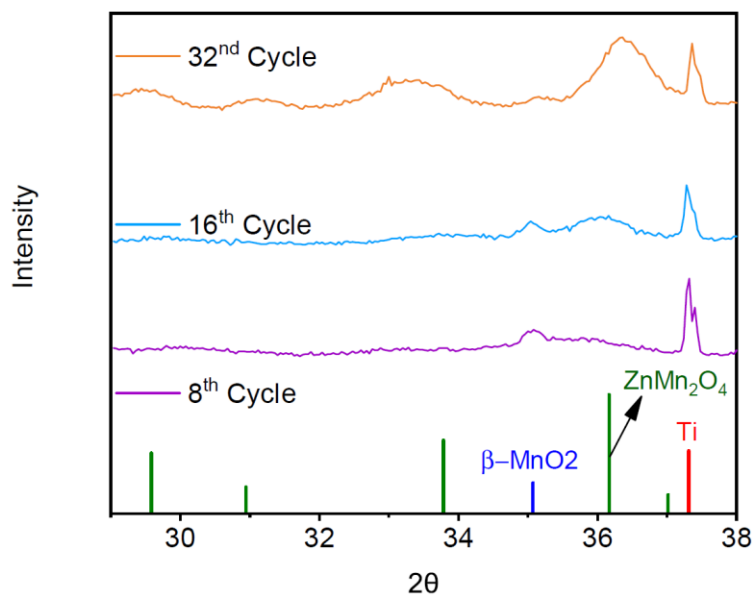


Fig. S 14 Laboratory XRD results indicating the growth of the irreversible hetaerolite phase, ZnMn₂O₄.

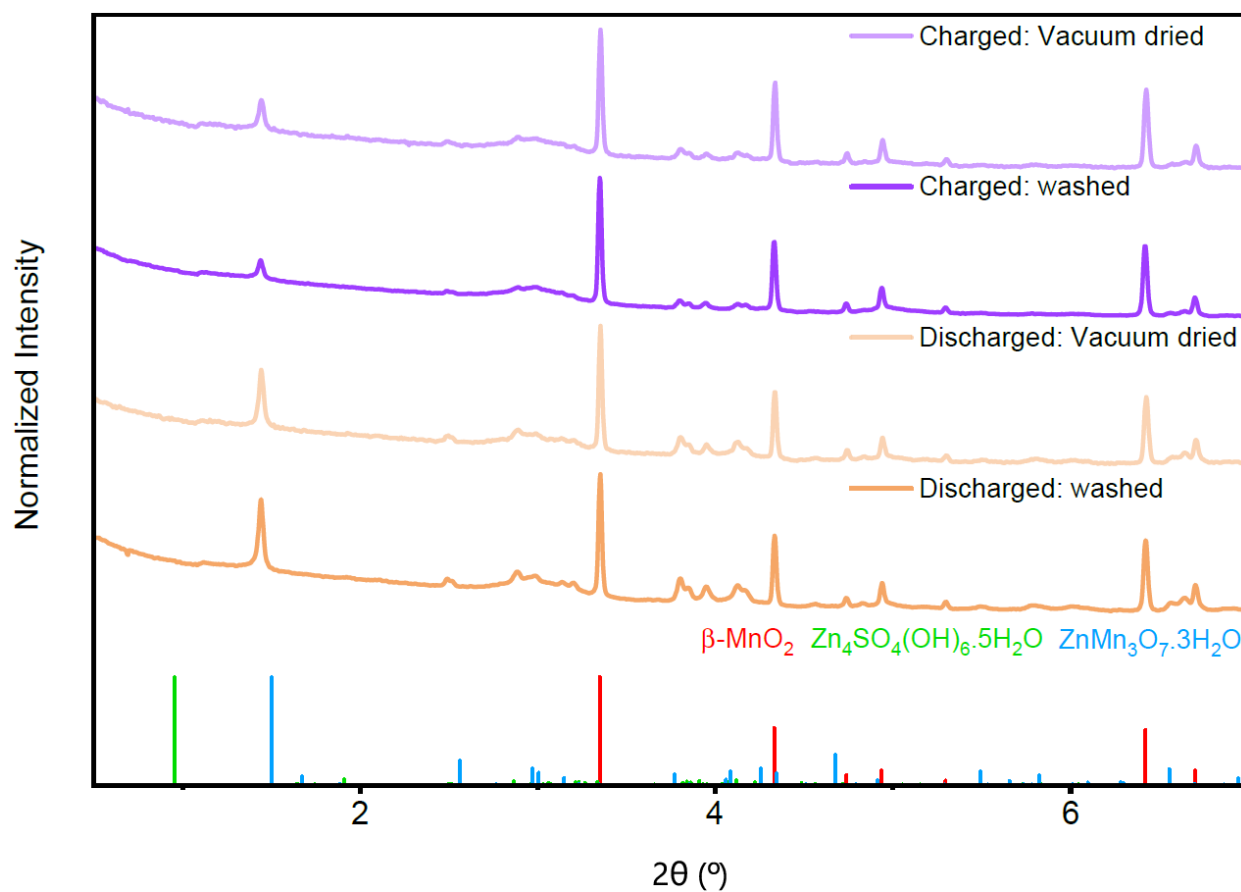


Fig. S 15 Synchrotron X-ray diffraction measurement of the electrode at discharge and charge state comparing the washed and the vacuum dried sample. The presence of the $\text{ZnMn}_3\text{O}_7 \cdot 3\text{H}_2\text{O}$ (Chalcofanite) phase is still visible.

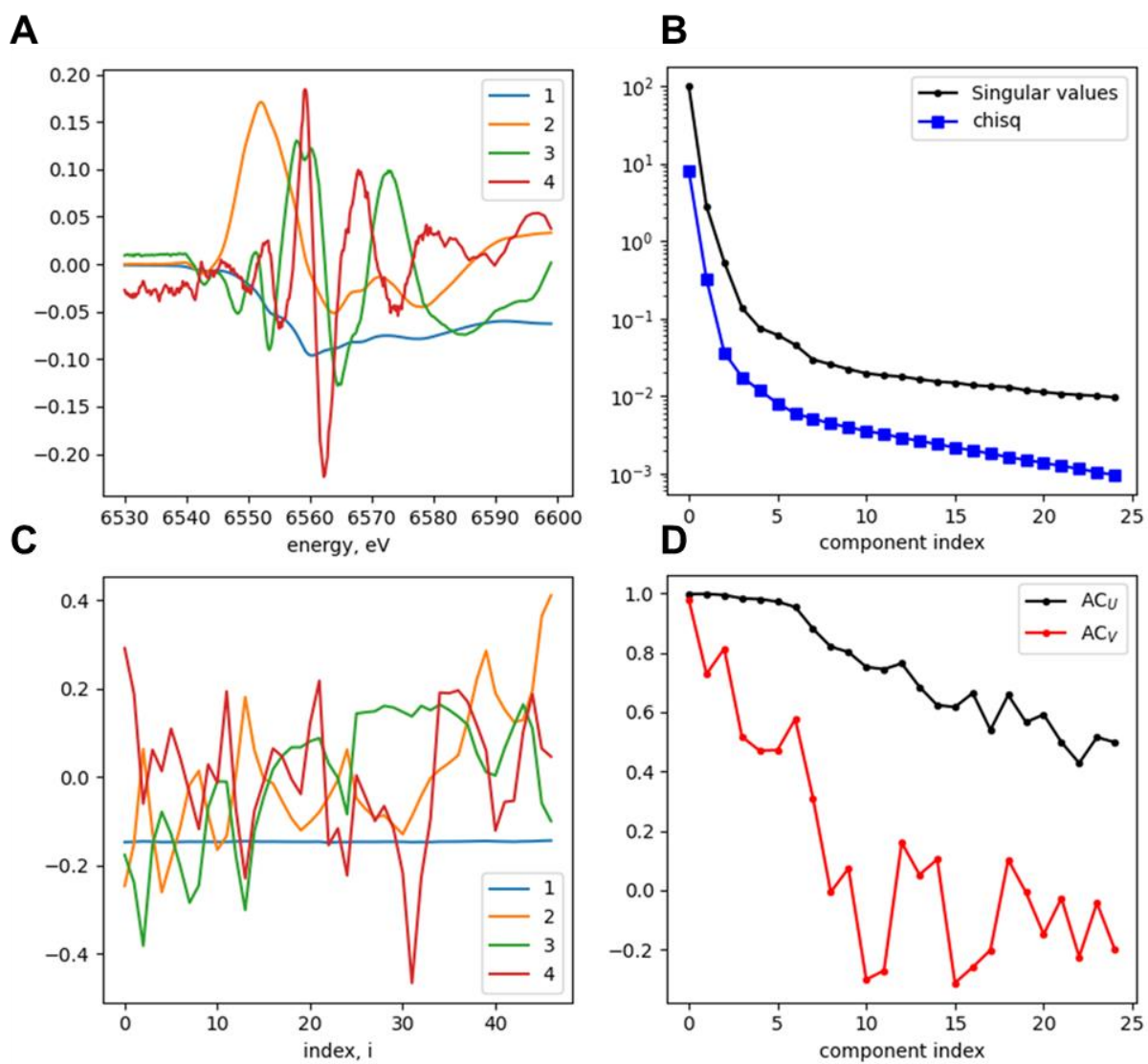


Fig. S 16 SVD/PCA of MnO₂ electrode *operando* experimental dataset across the Mn-edge. **A** shows plot of first four eigen-spectra/PC's while **C** shows first four eigen-concentration profiles. **B** shows scree plot for varying number of principal components and **D** shows autocorrelation for eigen-spectra (black) and eigen-concentration profiles (red).

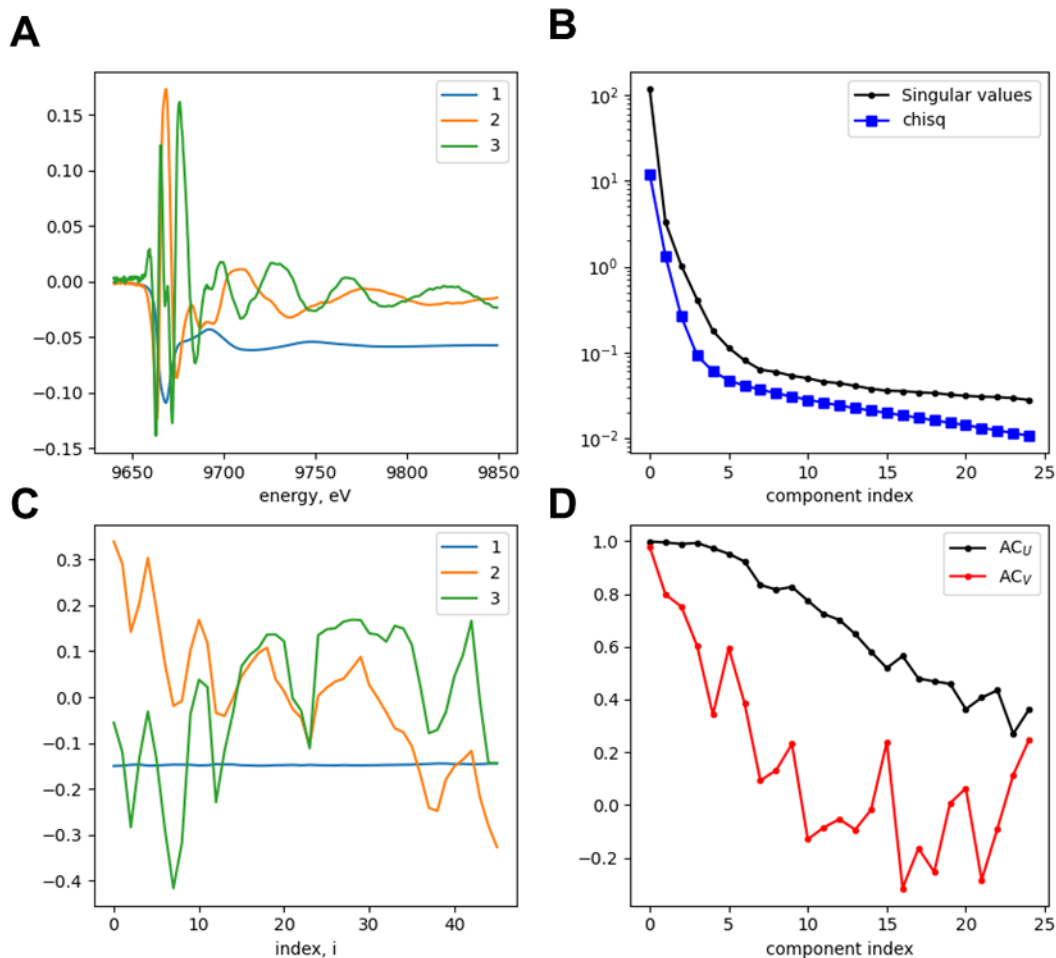


Fig. S 17 SVD/PCA of MnO₂ electrode *operando* experimental dataset across the Zn-edge. **A** shows plot of first four eigen-spectra/PC's while **C** shows first four eigen-concentration profiles. **B** shows screen plot for varying number of principal components and **D** shows autocorrelation for eigen-spectra (black) and eigen-concentration profiles (red).

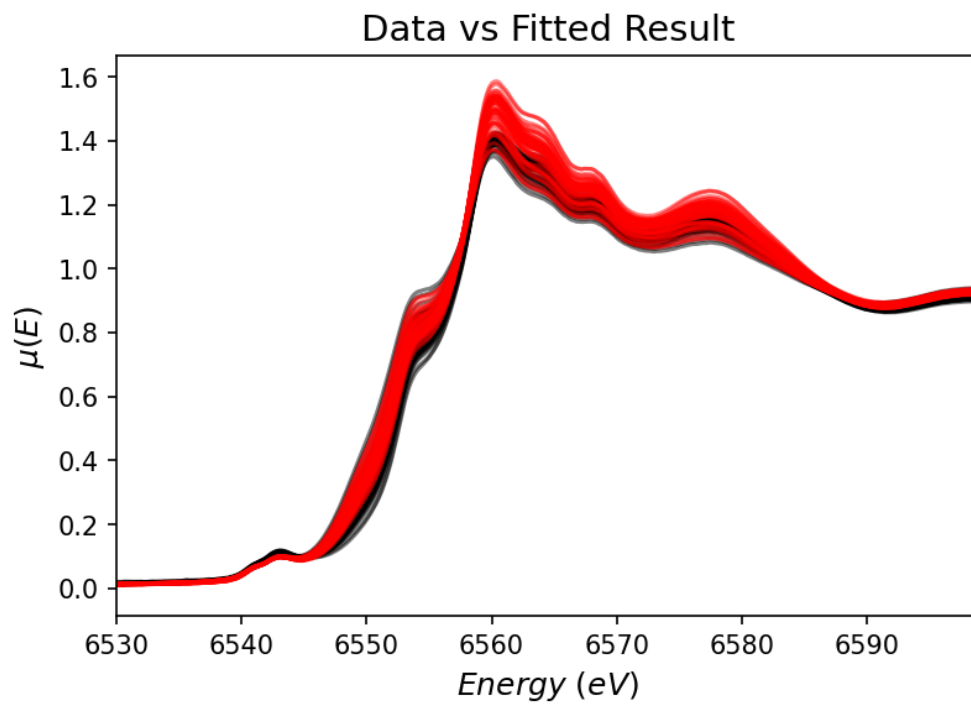


Fig. S 18 Fit result (in black) in comparison with the *operando* Mn-XANES dataset (in red).

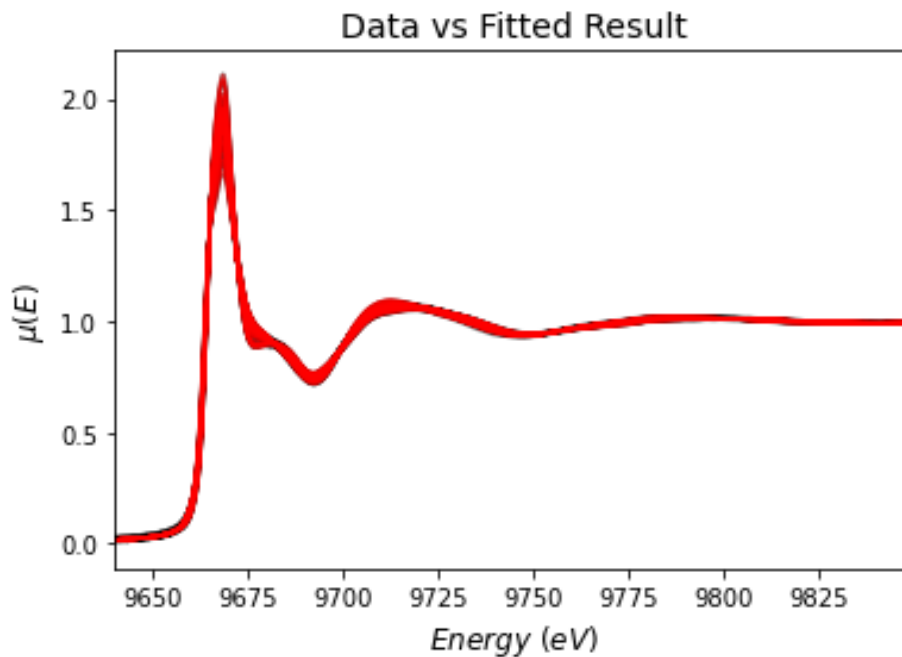


Fig. S 19 MCR-ALS fitting result (in black) in comparison with the *operando* Zn-XANES dataset (in red).

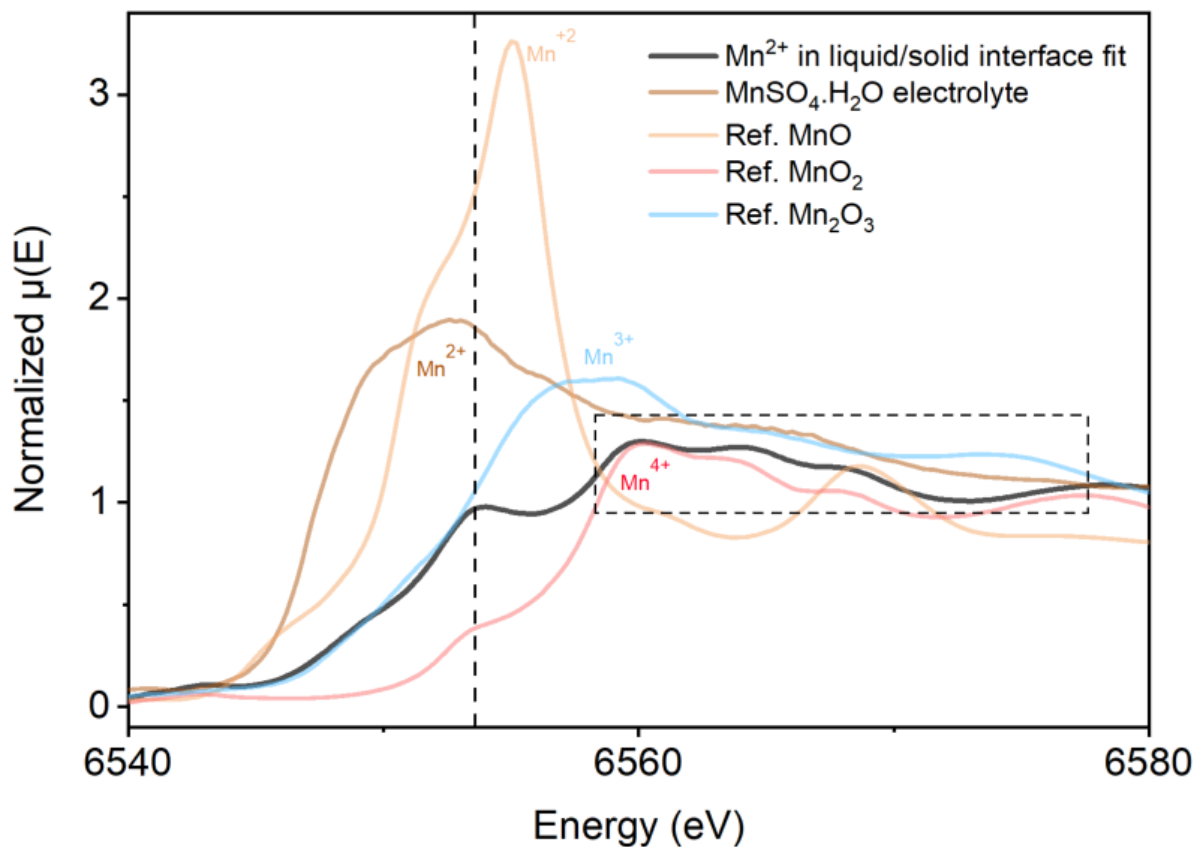


Fig. S 20 XANES spectra of Mn²⁺ in liquid/solid interface fit spectra, MnO₂, MnSO₄·H₂O, MnO, and Mn₂O₃ across the Mn-K edge. The dotted line indicates the contribution of the Mn²⁺ ions towards the pre-edge feature in the Mn²⁺ in liquid/solid interface fit spectra.

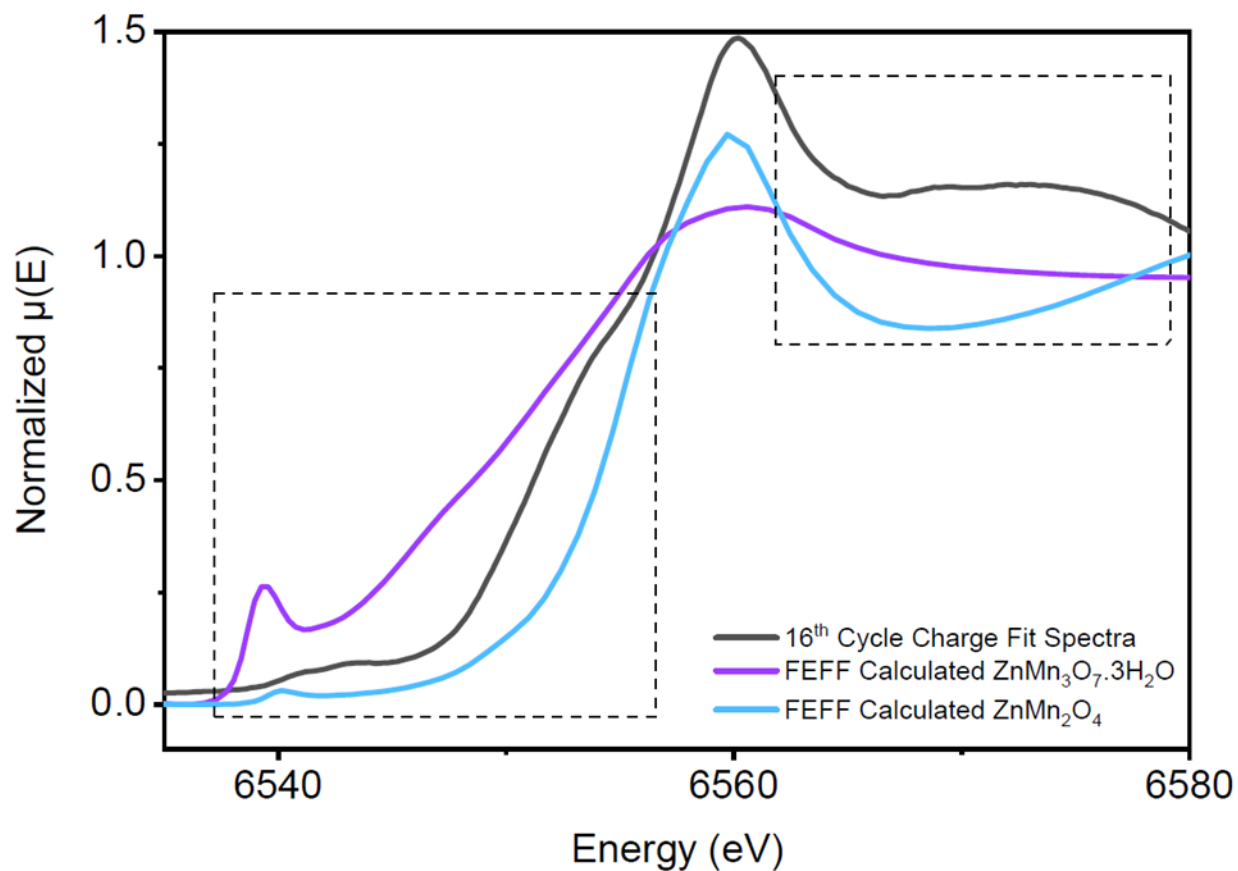


Fig. S 21 XANES spectra of MnO_2 16th cycle charge fit spectra, FEFF calculated $ZnMn_3O_7 \cdot 3H_2O$ and $ZnMn_2O_4$ across the Zn K-edge. The dotted boxes indicate the regions which are similar between the fitted spectra and the FEFF calculated spectra.

Supplementary Tables:

Table S1. A summary of samples that were characterized at different beamlines and instruments by extracting a portion of the same electrode.

Sample number	Sample Conditions	X-ray Diffraction	X-ray Absorption Spectroscopy	Transmission X-ray Microscopy	Field Emission Scanning Electron Microscope
1	1 st Cycle, Discharge @ 1.0 V		Y	Y	Y
2	1 st Cycle, Charge @ 1.75 V		Y	Y	Y
3	8 th Cycle, Discharge @ 1.0 V		Y	Y	
4	8 th Cycle, Charge @ 1.75 V	Y	Y	Y	Y
5	16 th Cycle, Discharge @ 1.0 V			Y	
6	16 th Cycle, Charge @ 1.75 V			Y	Y
7	32 nd Cycle, Charge @ 1.75 V	Y			Y

Table S2. The capacity likely associated with the amorphous phase, obtained from the difference of the total electrochemical capacity and the crystalline phase capacity. The total electrochemical capacity refers to the capacity obtained from the electrochemical cycling data. The crystalline phase capacity is obtained from the Rietveld Refinement of the *operando* X-ray diffraction scan as shown in **Fig. 2C**.

Cycle number	Total electrochemical capacity (mAh/g)	Crystalline phase capacity (mAh/g)	Amorphous phase capacity (mAh/g)
1	150	154	0
2	139.7	134.5	5.2
3	126.5	88	38.5

Table S3. Models that were evaluated for the MCR-ALS analysis of the *operando* XAS data across the Mn-edge, based on electrochemistry and the phase evolution. Different combinations of the spectra from different phases/states were used as initial guesses in the MCR-ALS analysis. The blue highlighted model (#10) was analyzed, and the concentration profiles were evaluated. The Zn-Mn complex corresponds to the XAS spectra across the Zn-edge obtained from the electrodeposited Zn-Mn phase on carbon cloth.

A four-component model was tried for testing the latter hypothesis, but this over constrained the model. Further refinement of the model would need to be physically validated to the fit spectrum results.

<i>Model No.</i>	<i>MnO₂</i>	<i>MnSO₄</i>	<i>Zn-Mn Complex</i>	<i>8-Cycle Charge</i>	<i>16-Cycle Charge</i>	<i>32-Cycle Charge</i>
1	Fix	Fix	Vary			
2	Fix	Fix		Vary		
3	Fix	Fix			Vary	
4	Fix	Fix				Vary
5	Fix	Vary	Vary			
6	Fix	Vary		Vary		
7	Fix	Vary			Vary	
8	Fix	Vary				Vary
9	Fix		Vary	Vary		
10	Fix		Vary		Vary	
11	Fix		Vary			Vary
12	Vary					Vary
13	Vary				Vary	
14	Vary		Vary			Fix
15	Vary	Vary	Vary			Vary
16	Fix	Fix	Vary			Fix

Table S4. Models that were evaluated for the MCR-ALS analysis, based on electrochemistry and the phase evolution from *operando* XAS data across the Zn-edge. Different combinations of the spectra from different phases/states were used as initial guesses in the MCR-ALS analysis. The blue highlighted model (#2) was analyzed, and the concentration profiles were evaluated. Zn-Mn complex corresponds to the XAS spectra across the Zn-edge obtained from the electrodeposited Zn-Mn phase on carbon cloth.

<i>Model No.</i>	<i>ZnSO₄</i>	<i>ZHS (1st Cycle discharge)</i>	<i>1st Cycle Charge</i>	<i>Zn-Mn Complex</i>	<i>8th Cycle Charge</i>
1	Vary	Vary	Vary		

2	Vary	Vary	Vary	
3	Vary	Vary		Vary
4	Vary	Vary		Fix
5	Vary	Vary	Vary	Vary
6	Vary	Vary	Vary	Fix
7	Vary	Vary		Fix

References:

1. K. Yan, Z. Lu, H.-W. Lee, F. Xiong, P.-C. Hsu, Y. Li, J. Zhao, S. Chu and Y. Cui, *Nature Energy*, 2016, **1**, 16010.
2. K. Momma and F. Izumi, *Journal of Applied Crystallography*, 2011, **44**, 1272-1276.